An attempt to determine a relationship between a mass-spring-friction damper single-degree-of-freedom system's equivalent viscous damping ratio and its corresponding friction coefficient

K. van Rensburg, S. Ramhormozian

Department of Built Environment Engineering, Auckland University of Technology, Auckland.

ABSTRACT

Damping forces are always present in real structures, occurring in several different forms, making them challenging to model expressly. Damping is often assumed to be viscous in nature, due to the simplicity of the mathematics, sometimes inappropriately when large friction forces are present.

This research aimed to determine a relationship between a friction-based single degree of freedom (SDOF) structure's assumed equivalent viscous damping ratio and the coefficient of friction.

This research focused on mathematically modelling the dynamic response of a theoretical single-storey structure, behaving linear elastically, to an applied harmonic load in two different damping cases namely the common assumption of viscously underdamped and a friction damping case, using an alternative approach that simplifies the traditionally non-linear solution to a linear one.

The physical model was idealised as an SDOF spring-mass-damper system and the mathematics of the general solutions for this system's responses to different damping cases and vibration types introduced. Notably covering the classic non-linear approach to friction damping, for comparison. The simplified response for the friction damped case under harmonic excitation, was derived from first principles by adapting a method proposed for free friction damped vibration.

The system's response for a range of common viscous damping ratios are analysed. The same analysis being performed for a range of different friction coefficients.

Ultimately the damping ratios and friction coefficients are compared, those causing similar responses from the system were selected, and a simple initial relationship between the viscous and friction damped cases determined for the selected cases.

1 INTRODUCTION

Simplification and idealisation of structural systems into simple spring-mass-damper systems is an effective method of analysing a structure's dynamics. Damping reduces oscillations or vibrations in a system, physical systems produce damping through processes that dissipate energy stored in the vibrations. Viscously damped SDOF systems are well studied in literature but most sources seem to shy away from friction damped SDOF systems.

Sliding friction is generated when two surfaces that press against each other are in relative motion or vibrating, dissipating kinetic energy into heat i.e. damping. This is generally called Coulomb damping after Charles-Augustin de Coulomb, here the frictional damping force always opposes the direction of motion of the system, creating a non-linear system that has a piecewise exact solution.

This paper starts by reviewing free as well as harmonically forced vibration of viscously and friction damped systems, looking at a method proposed by Rizcallah (2019) to simplify the mathematics of friction damping. For the forced vibration of the friction-based system, an expression is derived using the simplified method. The governing equations are numerically solved and plotted using MATLAB programming language.

1.1 Viscously damped SDOF

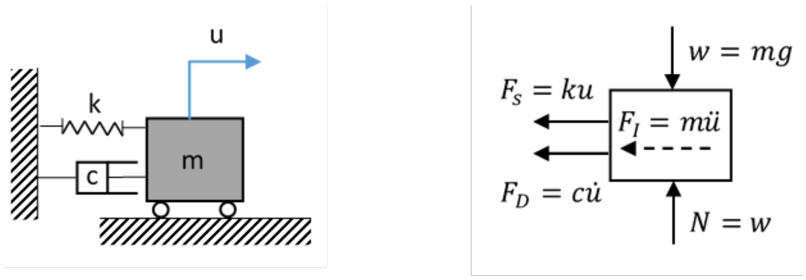

Figure 1: (a) Mass-spring-damper system sliding over a frictionless surface (b) Free-body diagram of the system in free vibration.

It is not possible to have a system that vibrates indefinitely with a constant amplitude at its natural frequency. Ever present frictional or damping forces dissipate energy, transforming the energy into other forms. How this energy transformation occurs is not yet fully understood.

In the dynamic analysis of structures, it is typically assumed that the damping forces within a structure or system act in the opposite direction of motion and are proportional to the system's velocity. This type of damping force could be experienced by a body that's motion is restrained by a viscous fluid which surrounds it.

Assuming viscous damping in a system is primarily used as it can often appropriately represent actual damping sources and because of the linearity and simplicity of its mathematics.

Figure 1(a) shows a SDOF mass-spring-damper system with no externally applied force, where c is the viscous damping coefficient, and the viscous damper is represented by a simple dashpot. Figure 1(b) shows the free-body diagram of the system with the damping force $F_D = c\dot{u}$ showing the assumption of proportionality between damping and velocity.

The full derivation of the general solution is covered in depth by Chopra (2017) and Ramhormozian (2020), and here only the final general solution for an underdamped system will be given.

As the damping coefficient for real structural systems has been found to be quite a bit smaller than their critical damping coefficient, the underdamped case of the general solution is the one of interest, given by the simplified expression:

$$\boldsymbol{u(t) = Ce^{-\xi\omega_n t}\cos(\omega_D t - \alpha)} \qquad (1)$$

Where $C = \sqrt{u_0^2 + \frac{(v_0+u_0\xi\omega_n)^2}{\omega_D^2}}$ and $\alpha = \tan^{-1}\left(\frac{(v_0+u_0\xi\omega_n)}{\omega_D u_0}\right)$

The system has a natural undamped frequency of ω_n, and at time $t = t_0$, the systems initial displacement and velocity are u_0 and v_0 respectively. ξ is the damping ratio of the system, calculated as $\xi = \frac{c}{c_{cr}}$, where c is the system's viscous damping coefficient and c_{cr} is its critical viscous damping coefficient.

Ramhormozian (2020) notes that real structures' damping ratios typically range between 2% and 10%.

The damped angular frequency of the system ω_D, given in $\frac{rad}{s}$, is calculated as

$$\boldsymbol{\omega_D = \omega_n\sqrt{1-\xi^2}} \qquad (2)$$

It follows that the damped period of vibration and damped frequency of the system are then $\boldsymbol{T_D = \frac{2\pi}{\omega_D}}$ and $\boldsymbol{F_D = \frac{1}{T_D}}$.

Equation 1 is graphically illustrated in Figure 2. The amplitude is observed to decrease exponentially with time, with the upper and lower envelope lines of the displacement-time curve described by the equations

$$\boldsymbol{u_{upper}(t) = Ce^{-\xi\omega_n t}} \qquad (3)$$
$$\boldsymbol{u_{lower}(t) = -Ce^{-\xi\omega_n t}}$$

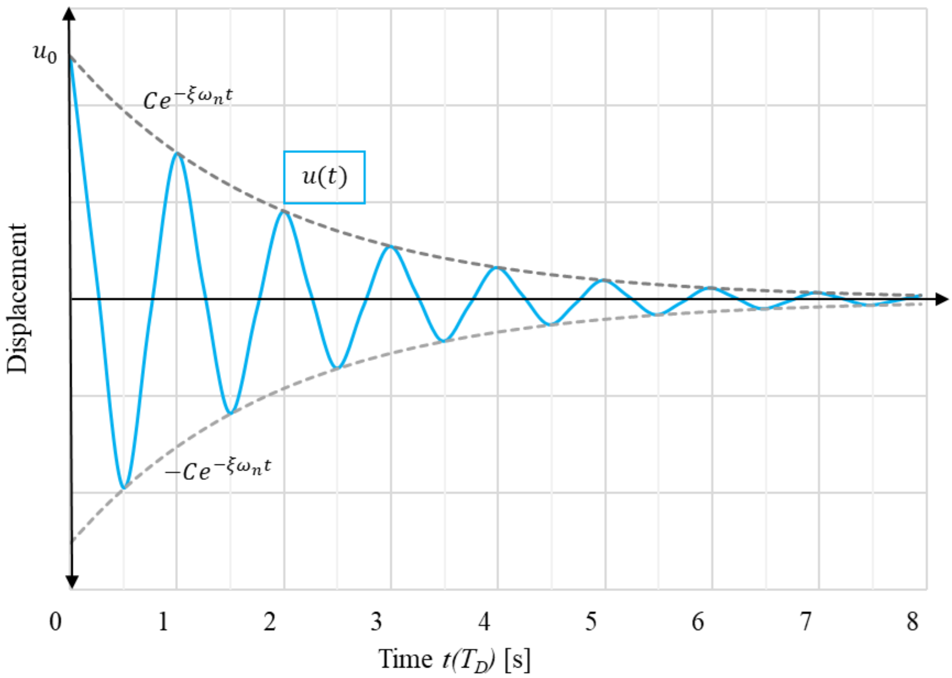

Figure 2: Displacement vs. time graph of the viscously underdamped system in free vibration.

1.2 Classically coulomb damped

This section first introduces piecewise expressions for friction or Coulomb damped free vibration as outlined by Chopra (2017). Then the next section looks at another method of defining friction as a harmonic force, proposed by Rizcallah (2019).

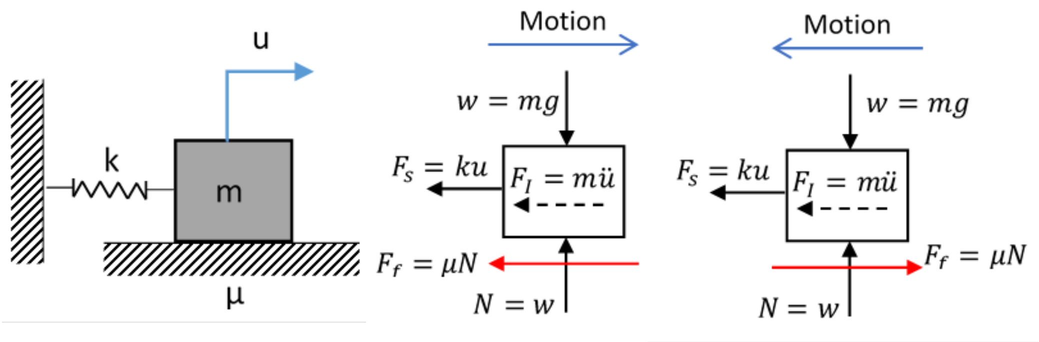

Figure 3: (a) Mass-Spring system sliding against a dry surface (b) & (c) Free-body diagrams of the system for both directions of motion.

Figure 3(a) shows a SDOF mass-spring system where the mass is sliding against a dry surface that has the dimensionless friction coefficient μ. Coulomb damping results from this friction force, $F_f = \mu N$, where N is the normal force between the sliding surfaces and μ is assumed the same for static and kinetic friction. The assumption is that once motion begins, friction is independent from velocity, differing from viscous damping explained previously. Friction acts in opposition to motion, changing direction or sign when the motion changes direction.

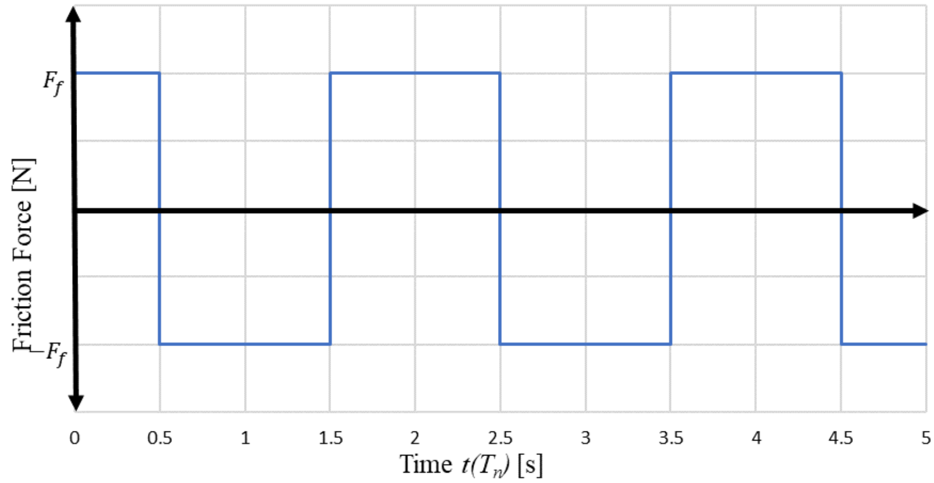

Figure 4: Friction force vs. time graph illustrating period alternation of friction with every half-cycle.

Assuming that the motion of system is periodic, the friction force vs time is as seen in Figure 4 above, changing direction with every half-cycle.

Chopra (2017) noted that the natural period of a system that is Coulomb damped is equal to that of the same system without damping, while viscous damping lengthens the natural vibration period.

Because of the nature of friction discussed above, two different equations of motion need to be formulated and solved, valid for a specific direction of motion. This section looks at when the system in Figure 3(a) is freely vibrating and there is no externally applied force i.e. $F(t) = 0$. The equation of motion that governs when the mass in Figure 3(c) is moving right to left is given in Equation (***4)*** below

$$\boldsymbol{m\ddot{u} + ku = F_f} \tag{4}$$

the solution to which is

$$\boldsymbol{u(t) = A_1\,cos(\omega_n t) + B_1\,sin(\omega_n t) + u_F} \tag{5}$$

where $u_F = \frac{F}{k}$ .When the mass moves left to right, as seen in Figure 3(b), the governing equation changes to

$$\boldsymbol{m\ddot{u} + ku = -F_f} \tag{6}$$

and its solution is

$$\boldsymbol{u(t) = A_2\,cos(\omega_n t) + B_2\,sin(\omega_n t) - u_F} \tag{7}$$

The constant u_F and $\omega_n = \sqrt{\frac{k}{m}}$ are interpreted by Chopra (2017) as the spring's static deformation caused by the friction force F_f. The arbitrary constants $A_1, B_1; A_2, B_2$ are found from the initial conditions, which change for each successive half-cycle of motion. Because of this, the linear governing equations change with every half-cycle of motion, creating a non-linear problem.

For some given initial conditions, $t_0 = 0, u(t_0) = u_0, \dot{u}(t_0) = v_0 = 0$, the system in Figure 3(a) will vibrate freely until it comes to rest and stops moving. For brevity, in this paper the generalised equations given in Rizcallah (2019) are used instead of more complicated solution presented in Chopra (2017).

the general solution to the system's displacement response over time is

$$\boldsymbol{u(t) = (u_0 - (1 + k_n)u_F)\,cos(\omega_n t) + (-1)^n u_F} \tag{8}$$

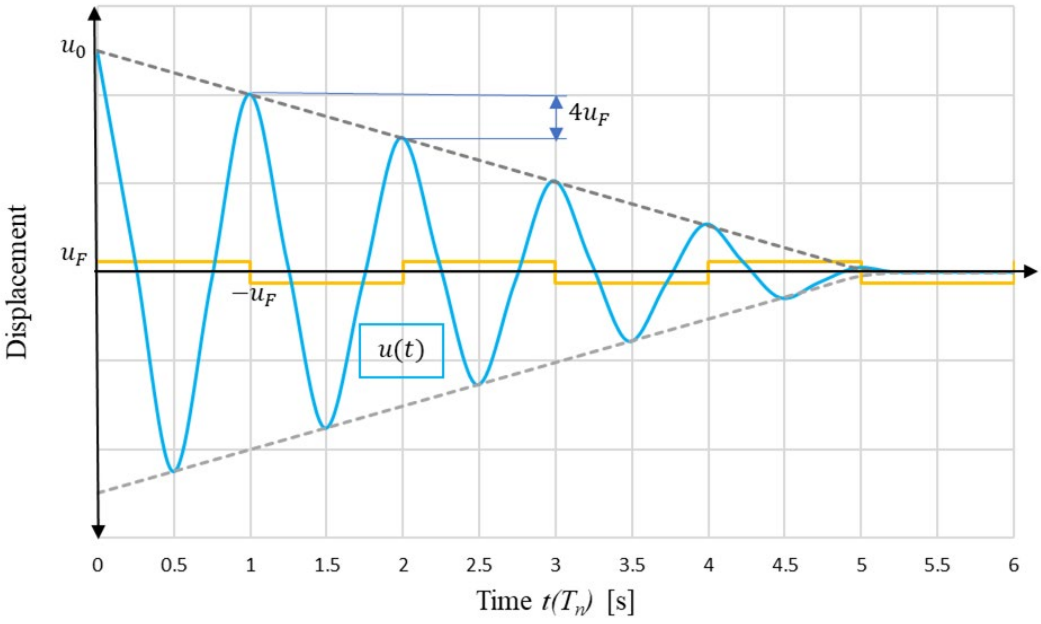

Figure 5: Displacement vs time graph of the free vibrating system with Coulomb damping.

The displacement response of the system in Figure 3(a) is shown in Figure 5. Observe that, with each motion cycle, the amplitude reduces by $4u_F$ meaning that the envelopes are linear functions as opposed to exponential in the case of viscous damping. The equations of which are easily determined as

$$\boldsymbol{u_{upper}(t) = -\left(\frac{4u_F}{T_n}\right) + u_0} \quad (9)$$

$$\boldsymbol{u_{lower}(t) = \left(\frac{4u_F}{T_n}\right) - u_0}$$

Coulomb damping of a freely vibrating system causes its motion to stop when the amplitude at the end of a half-cycle is less than u_F. This means that the friction force is greater than the spring force acting on the mass. The end condition for free vibration of a Coulomb damped system is given by the inequality

$$\boldsymbol{F_s = k|u(t)| < F_f = \mu N} \quad (10)$$

for any time t.

Note that the final resting of the mass is not at its original equilibrium position but at a different position. This displacement is a permanent deformation where the spring force and friction force are locked in and the system would need externally applied energy such as jarring or shaking to restore it to equilibrium.

Coulomb damping must play a role in damping of real structures explains Chopra (2017), especially as this is the only mechanism that can halt the motion of a freely vibrating system. Chopra (2017) notes that if damping in structures was purely viscous, their motion would theoretically continue forever at ever tinier amplitudes, see Figure 2. Although Coulomb damping must exist in structures, it is not often considered, unless friction damping devices are used in structure.

Equivalent viscous damping ratios can be obtained to approximate dynamic responses, this is probably due to the lack of knowledge around friction damping and the non-linearity of its nature when compared to viscous damping's simple linear formulation. Rizcallah (2019) proposed an alternative solution to Coulomb damping, that would simplify the mathematics, this is explained in the next section.

1.3 Equivalent harmonic friction damping force

As previously explained, the frictional damping force always opposes the direction of motion of the system, creating a non-linear system that has a piecewise exact solution. Sliding friction has a constant magnitude, independent of the system's velocity, displacement or surface area and is often replaced by the linear viscous damping model in vibrations.

Rizcallah (2019) proposed to approximate the Coulomb friction force with an appropriate harmonic, specifically sinusoidal, resistive force.

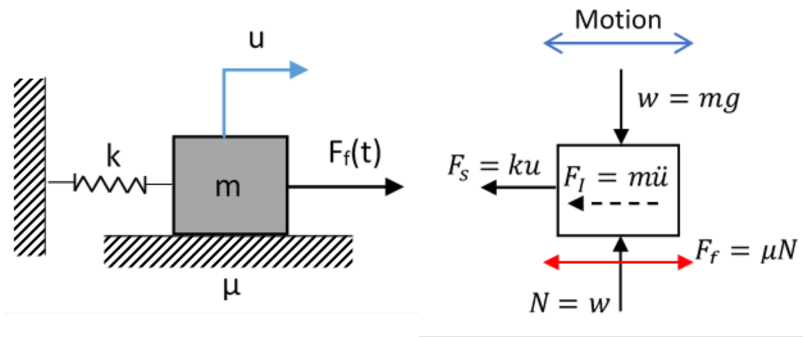

Figure 6: (a) Mass-Spring system sliding against a dry surface (b) Free-body diagram of the system.

To begin with, Rizcallah (2019) modifies the equation of motion shown in Equation (***11*** for Figure 6(b), which combines the two cases of motion from Equations (***4*** and (***6***

$$m\ddot{u} + ku = \pm F_f \tag{11}$$

By replacing the right-hand side with a sinusoidal resistive force

$$m\ddot{u} + ku = F\,sin(\omega_F t) \tag{12}$$

Figure 7(a) and (b) shows the new system created by replacing the friction force with an equivalent harmonic force.

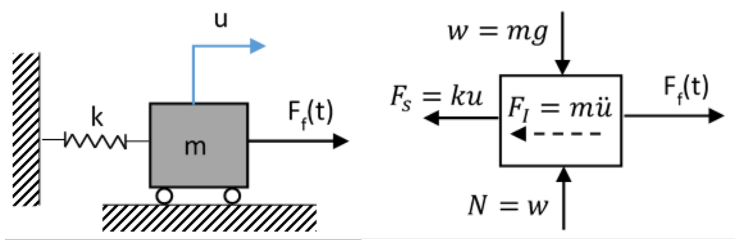

Figure 7: (a) Mass-Spring system with an externally applied equivalent harmonic friction force (b) Free-body diagram of the system.

The equivalent force has a forcing angular frequency of ω_F. Euler's equations allow the solution to follow an initial value problem, yielding a general solution of displacement, similar to that obtained from the forced harmonic excitation of an undamped system.

$$u(t) = A cos(\omega_n t) + B sin(\omega_n t) - \frac{\frac{F}{m}}{{\omega_F}^2 - \omega_n^2} sin(\omega_F t) \tag{13}$$

Initial conditions of $t_0 = 0, u(t_0) = u_0, \dot{u}(t_0) = v_0 = 0$ are used to solve the arbitrary constants

$$A = u_0$$
$$B = \frac{F\omega_F}{m\omega_n({\omega_F}^2 - \omega_n^2)} \tag{14}$$

Such that substituting these into Equation (*13* gives

$$u(t) = u_0 cos(\omega_n t) + \left(\frac{F\omega_F}{m\omega_n({\omega_F}^2 - \omega_n^2)}\right) sin(\omega_n t) - \frac{\frac{F}{m}}{{\omega_F}^2 - \omega_n^2} sin(\omega_F t) \tag{15}$$

Taking the limit $\omega_F = \omega_n$ of Equation (*15* or $\lim_{\omega_F \to \omega_n} u(t)$ yields

$$u(t) = u_0 cos(\omega_n t) + \left(\frac{F}{2m\omega_n^2}\right) sin(\omega_n t) - \left(\frac{F\omega_n t}{2m\omega_n^2}\right) cos(\omega_n t) \tag{16}$$

Simplifying Equation (*16* by substituting $k = m\omega_n^2$ and collecting like terms gives

$$u(t) = \left(u_0 - \frac{F}{2k}\omega_n t\right) cos(\omega_n t) + \frac{F}{2k} sin(\omega_n t) \tag{17}$$

Equation (*18* is illustrated in Figure 8 and here Rizcallah (2019) notes that the decay of motion is due to the resonance between the sinusoidal resistive force and the mass-spring system. If this solution is extrapolated further than the halting point, where the spring force is no longer greater than the frictional force, then an increasing oscillation is observed in Figure 8, which is an impossibility in a freely vibrating system.

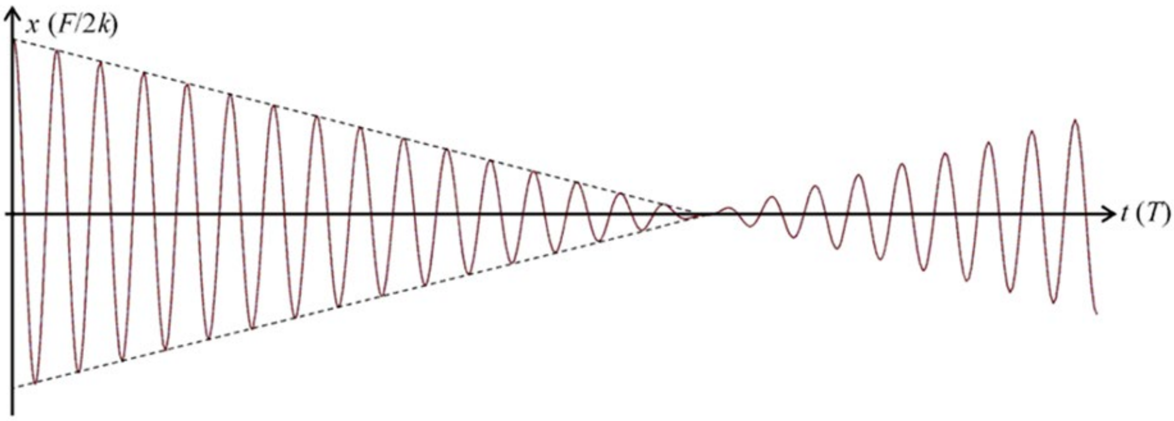

Figure 8: Illustration of the damped oscillations of a mass-spring system with a sinusoidal resistive force (Rizcallah, 2019).

Rizcallah (2019) argues and proposes that the analytical solution to Equation (*12)* that best fits the frictionally underdamped solution to Equation (*11)* is

$$\boldsymbol{u(t)} = \left(\boldsymbol{u_0} - \frac{\boldsymbol{2F_f}}{\boldsymbol{\pi k}}\boldsymbol{\omega_n t}\right)\boldsymbol{cos(\omega_n t)} + \frac{\boldsymbol{2F_f}}{\boldsymbol{\pi k}}\boldsymbol{sin(\omega_n t)} \tag{18}$$

where $F_f = \mu N$ is the friction force.

Figure 9 compares the two results of free vibrating systems considering equivalent friction harmonic force and non-linear coulomb damping, showing good correlation. The equations of the upper and lower envelope lines remain the same as seen in Equation (***9***.

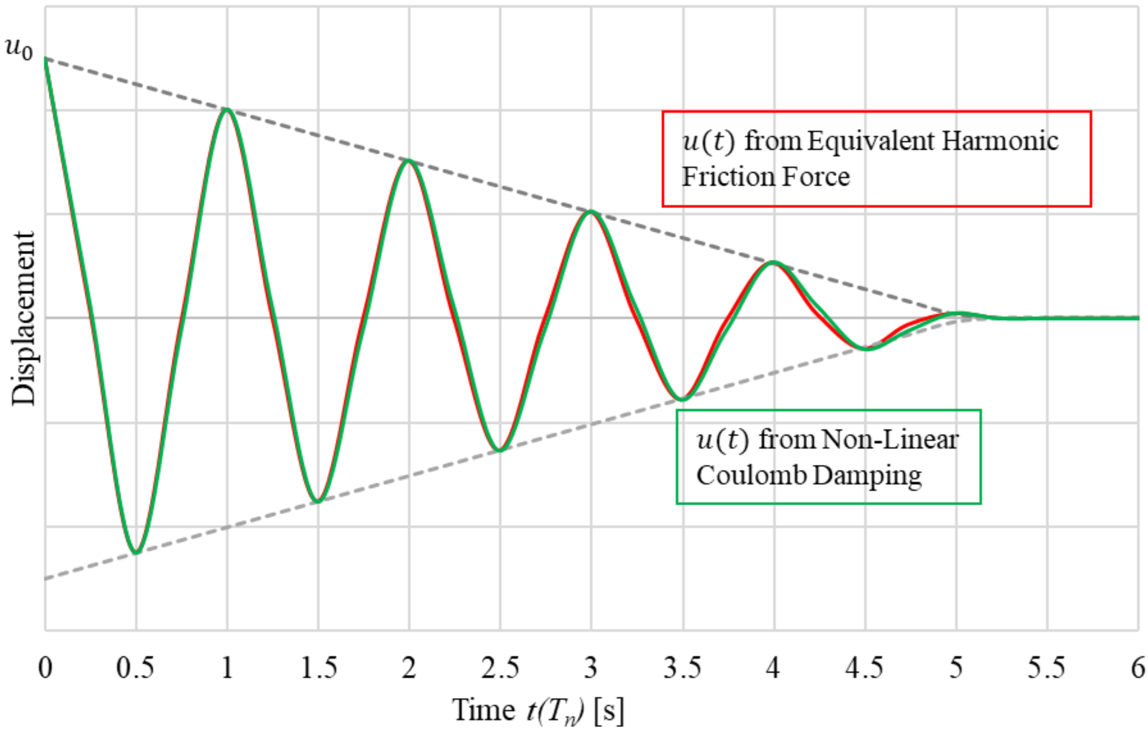

Figure 9: Displacement vs time graph of the free vibrating system comparing the two different solutions to frictional damping.

2 CASE STUDY

2.1 Physical model

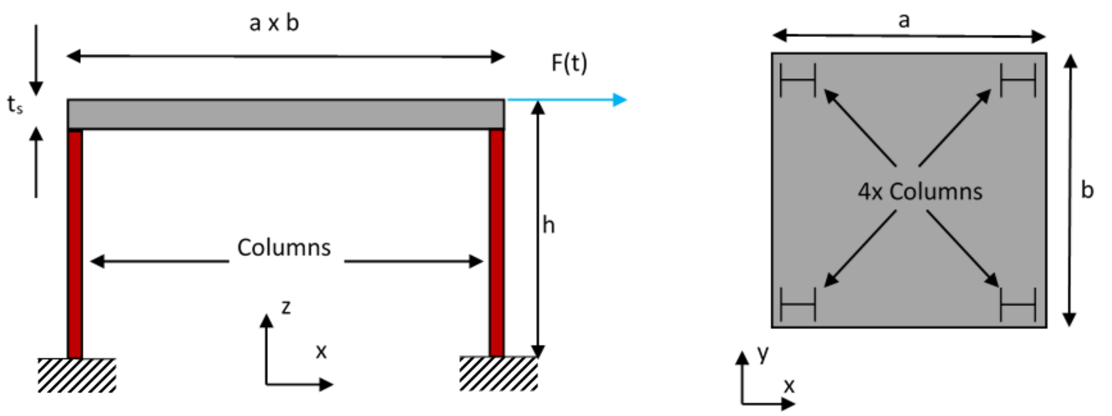

Figure 10: Physical model of the structural system under consideration

The physical model is a typical 1-storey composite structure, with a reinforced concrete roof slab and four structural steel columns. The columns are fixed at the base and rigidly connected to the slab. The dimensions, material properties and constants used are outlined in Table 1.

2.2 Assumptions

- The model is assumed to behave linear elastically.
- The roof slab is considered as a lumped mass.
- The roof slab is considered as a rigid, so rotations at the joints are eliminated.
- The column self-weight is negligible in this analysis as slab's self-weight is much greater and will govern the vibration response.
- Axial deformations in the beams and columns are neglected.
- Initially only classical viscous damping is assumed present in the structure.
- Then only Coulomb or friction damping is assumed present.
- The structure is an underdamped system
- The normal force is 100% of the system's mass.

Physical model's parameters are presented in below

Table 1: Physical model's (see Figure 10) parameters

Property	Symbol	Value	Unit
	Concrete Slab		
Density	ρ_{conc}	2400	kg/m^3
Length	a	2	m
Breadth	b	2	m
Thickness	t_{slab}	300	mm
	Steel Columns (IPE180 Sections)		
Density	ρ_{steel}	7850	kg/m^3
Length	L	2	m
Young's Modulus	E_{steel}	210	GPa
Moment of Inertia about y-y	I_{yy}	1320 (Tube, 2017)	mm^4
	Constants		
Gravitational Acceleration	g	9.81	m/s^2
	Initial Conditions		
Time	t_0	0	s
Displacement	u_0	5	mm
Velocity	$\dot{u}_0$ or v_0	0	m/s
Acceleration	$\ddot{u}_0$ or a_0	0	m/s^2
External Force	F_0	10	kN

2.3 Model idealisation

The analysis focused on the physical model's lateral vibration in the x-direction, see Figure 10. For analysis, this structure is simplified into a system consisting of a single lumped mass, springs for its columns and either a viscous or friction damper to represent the inherent internal damping forces within the structure. shows this idealisation and how the structure is further simplified into simple lollipop models, clearly showing that system has only a single degree of freedom in these simplifications.

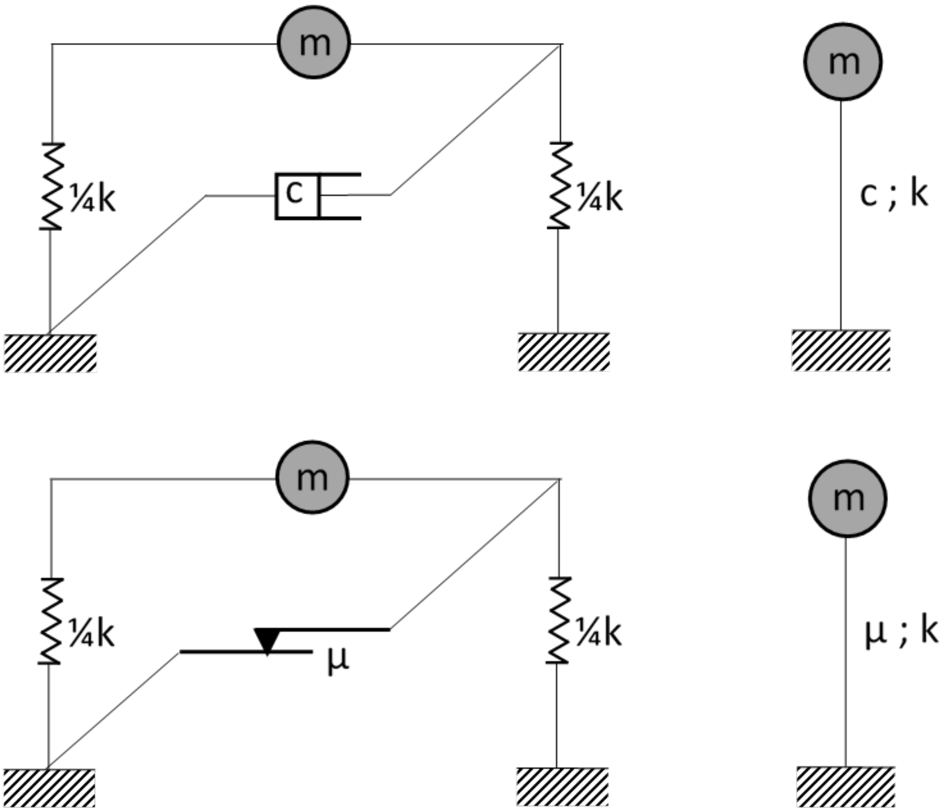

Figure 11: Idealisation of the physical model's structural frame and associated "lollipop" models for the viscous and equivalent friction damped cases.

The free-body diagrams for the lollipop models in Figure 11 of the two damping cases are given by Figures Figure 2 and Figure 12 for the viscous and equivalent friction damped cases respectively.

2.4 Mathematical derivation – harmonic excitation with equivalent harmonic friction damping

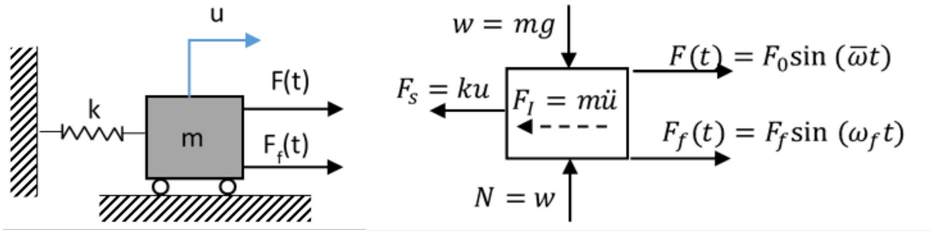

Figure 12: (a) Mass-spring system that is harmonically excited and subject to a harmonic friction force (b) Free-body diagram of the system with the two harmonic forces acting on it.

The dynamic equilibrium equation for vibration in the horizontal axis of the system, shown above in Figure 12(a), is determined from the free-body diagram, seen in (b), to be

$$m\ddot{u} + ku = F_0 \sin(\bar{\omega}t) + F \sin(\omega_f t) \tag{19}$$

To find the general solution to this equation, it is broken up into more manageable pieces and then solved individually. The solutions added together at the end using the principle of superposition.

Hence the general solution to Equation 19 becomes

$$u(t) = \left(u_0 - \frac{2F_f\omega_n t}{k\pi}\right)\cos(\omega_n t) + \left(\frac{v_0}{\omega_n} + \frac{2F_f}{k\pi} - \frac{rF_0}{k(1-r^2)}\right)\sin(\omega_n t) + \frac{F_0}{k(1-r^2)}\sin(\bar{\omega}t) \tag{20}$$

The expression in Equation 20 is expanded and each of the terms individually plotted to determine their contributions to the system's vibration. This helped to confirm what the expressions of the transient response of the system, determined to be

$$u_{transient}(t) = \left(u_0 - \frac{2F_f\omega_n t}{k\pi}\right)\cos(\omega_n t) + \left(\frac{v_0}{\omega_n} + \frac{2F_f}{k\pi}\right)\sin(\omega_n t) \tag{21}$$

Where the friction force is $F_f = \mu N$.

The steady-state response term is then made up of the remaining terms, becoming

$$u_{steadystate}(t) = \frac{F_0}{k(1-r^2)}\left(\sin(\bar{\omega}t) - r\sin(\omega_n t)\right) \tag{22}$$

The steady-state term in Equation 22 is not a constant and smooth sinusoidal curve when plotted, unlike in the case of un-damped or viscously damped. Figure 13 illustrates the individual sinusoidal curves that make up the oddly stepped superimposed curve of the steady-state response.

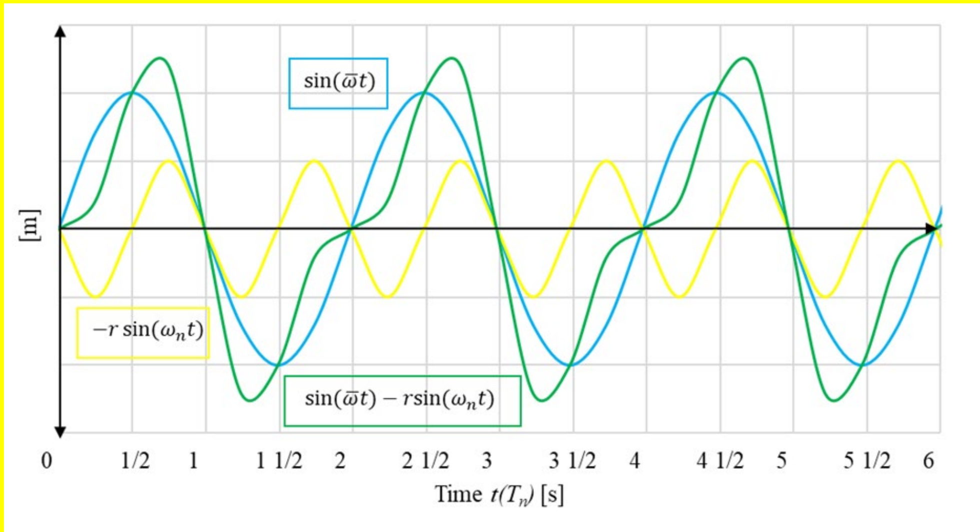

Figure 13: Illustration of the behaviour of the steady-state term's sinusoidal components in (3.5.1.19).

Therefore, the total response of a harmonically excited and frictionally damped system, using an equivalent harmonic friction force, shown in Figure 12(a), is given as:

$$\boldsymbol{u(t) = \left(u_0 - \frac{2F_f\omega_n t}{k\pi}\right) cos(\omega_n t) + \left(\frac{v_0}{\omega_n} + \frac{2F_f}{k\pi}\right) sin(\omega_n t) + \frac{F_0}{k(1-r^2)}\left(sin(\bar{\omega}t) - r\, sin(\omega_n t)\right)} \tag{23}$$

Equation (***23)*** is illustrated in Figure 14, the transient response displaying the expected characteristic of eventually disappearing over time and the steady-state response constantly oscillating as expected, but in the unusual, stepped curve behaviour discussed previously.

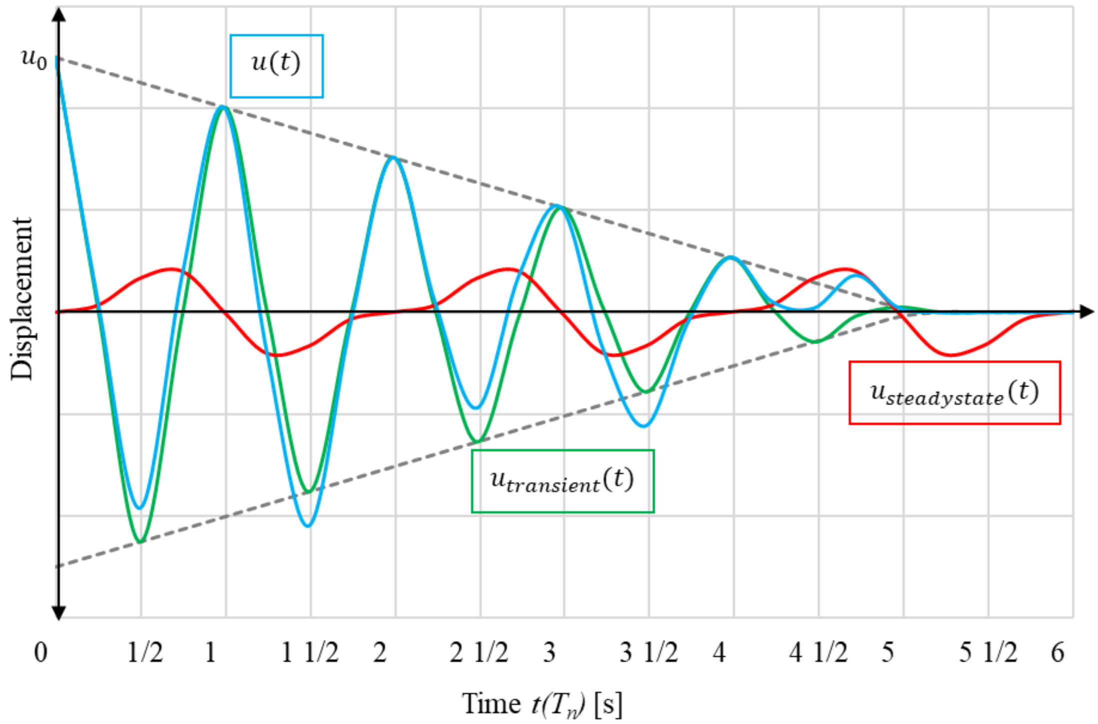

Figure 14: Displacement vs time graph of a harmonically excited system with an equivalent harmonic friction damping force.

The velocity response of the system is given by taking the first derivative of displacement with respect to time, yielding

$$\dot{u}(t) = \left(\frac{v_0}{\omega_n}\right)\omega_n\, cos(\omega_n t) - \left(u_0 - \frac{2F_f}{k\pi}\omega_n t\right)\omega_n\, sin(\omega_n t) + \frac{F_0}{k(1-r^2)}\left(\bar{\omega} cos(\bar{\omega} t) - \omega_n r\, cos(\omega_n t)\right) \tag{24}$$

The acceleration response, from taking the second derivative of displacement with respect to time, is

$$\ddot{u}(t) = \left(\frac{2F_f}{k\pi} - \frac{v_0}{\omega_n}\right)\omega_n^2\, sin(\omega_n t) - \left(u_0 - \frac{2F_f}{k\pi}\omega_n t\right)\omega_n^2\, cos(\omega_n t) + \frac{F_0}{k(1-r^2)}\left(\omega_n^2 r\, sin(\omega_n t) - \bar{\omega}^2\, sin(\bar{\omega} t)\right) \tag{25}$$

2.5 Model Solution Procedure

For the harmonically excited and damped SDOF model:

1. Calculate system's mass m and lateral stiffness k from the given parameters.
2. Calculate the system's natural vibration characteristics.

For the viscous damped case:

3. Assume a viscous damping ratio ξ.
4. Calculate the system's damped vibration characteristics.
5. Calculate the constants for the vibration response of the system from initial conditions.
6. Calculate the system's displacement response, as well as velocity and acceleration responses over a set period, at chosen intervals of $\frac{T_D}{16}[s]$.

For the equivalent friction damped case:

3. Assume a friction coefficient μ.
4. Calculate the normal N and friction forces F_f acting on the system.
5. Calculate the system's displacement, velocity, and acceleration responses - using Equations (***23)***, (***24)*** and (***25)*** respectively and the given initial conditions, over a set period and at chosen intervals of $\frac{T_D}{16}[s]$.

3 RESULTS

3.1 Responses

3.1.1 Viscous damped

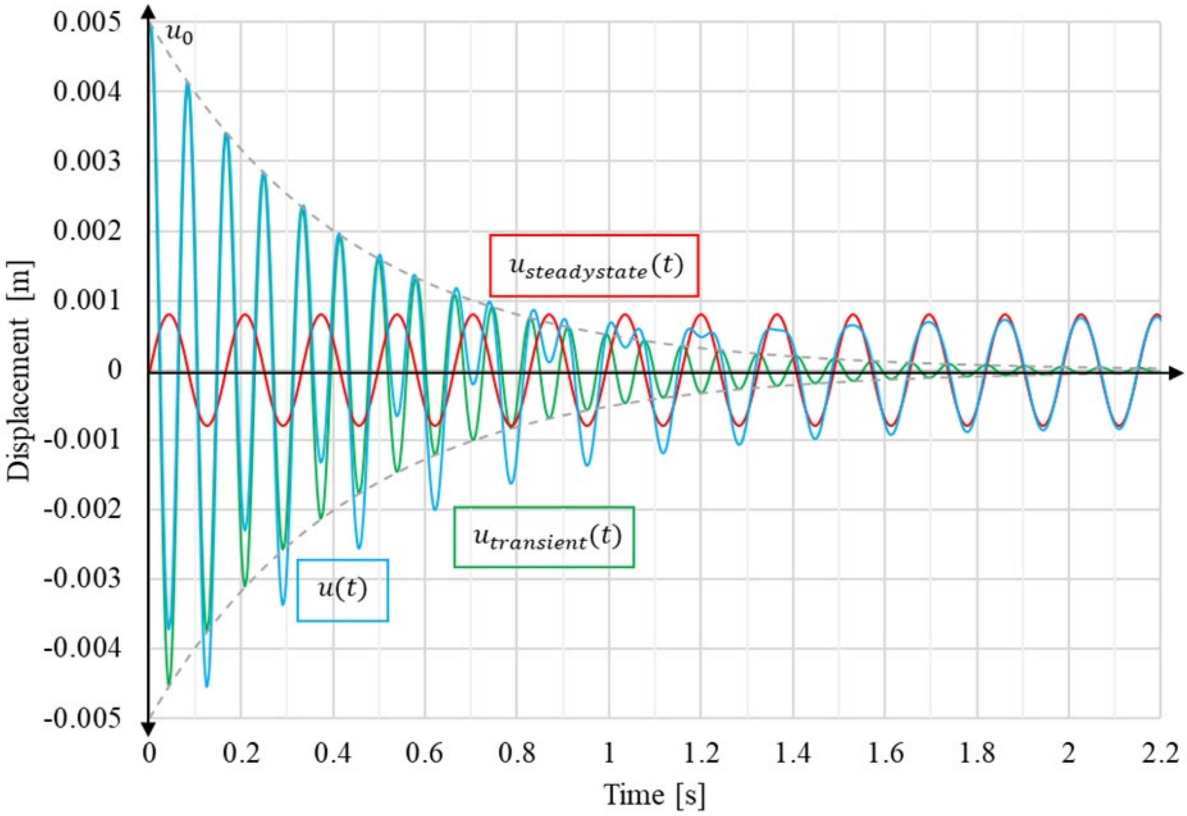

Figure 15: Displacement response of harmonically excited and viscously damped physical model with ξ=3%

The model's responses in the viscous damping case, for all the different values of ξ, display the expected behaviour. The transient displacement response reducing exponentially, shown by the envelopes, eventually disappearing.

The steady-state displacement response remains constant, with smooth sinusoidal curves, the same for all the different values of ξ.

As the viscous damping ratio increases, the model's transient response returns to rest sooner, this can be seen in Figure 18 which compares all the different damping values.

3.1.2 Equivalent friction damped

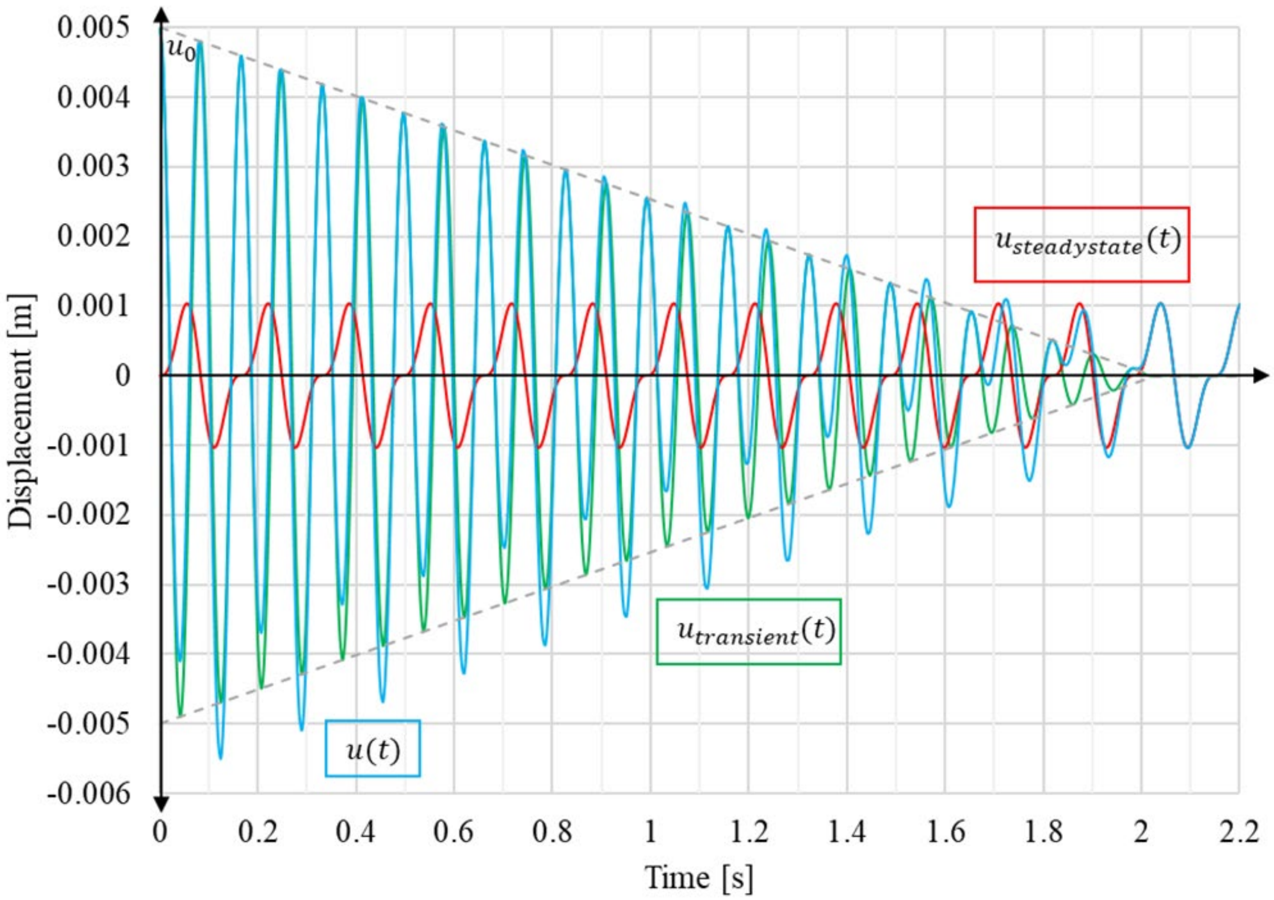

Figure 16: Displacement response of harmonically excited and equivalent friction damped physical model with μ=0.03

The model's transient displacement responses in this damping case, for all the different μ values, behaved in the expected manner. The transient displacement envelope confirms this behaviour of linearly decreasing peaks, typical of classic Coulomb damping in free vibration and emulated by the equivalent harmonic friction damping method discussed previously in Section 1.3 of this paper.

As the friction coefficient increases, the model's transient response decreases quicker, coming to rest sooner, see Figure 18.

Figure 17 confirms that the transient displacement, velocity and acceleration responses of the equivalent friction damped model behave as expected of harmonic curves. Their respective peaks, zero points and troughs being separated by $\frac{\pi}{2}\ rad$ from one another.

However, as noted in the derivation of the steady-state expression in Section 2.4, the model's steady-state displacement responses, the same for all the different μ values, display as constant "stepped" sinusoidal curves.

This is as opposed to the smooth steady-state response curves seen in Figure 15, the viscous damping case. Note the larger amplitude of the steady-state response in the friction damped case, resulting in total displacement response peaks greater than the initial displacement condition between 0.1s and 0.3s. The amplitude of the steady-state response remains constant as the friction coefficient value increases, which is expected.

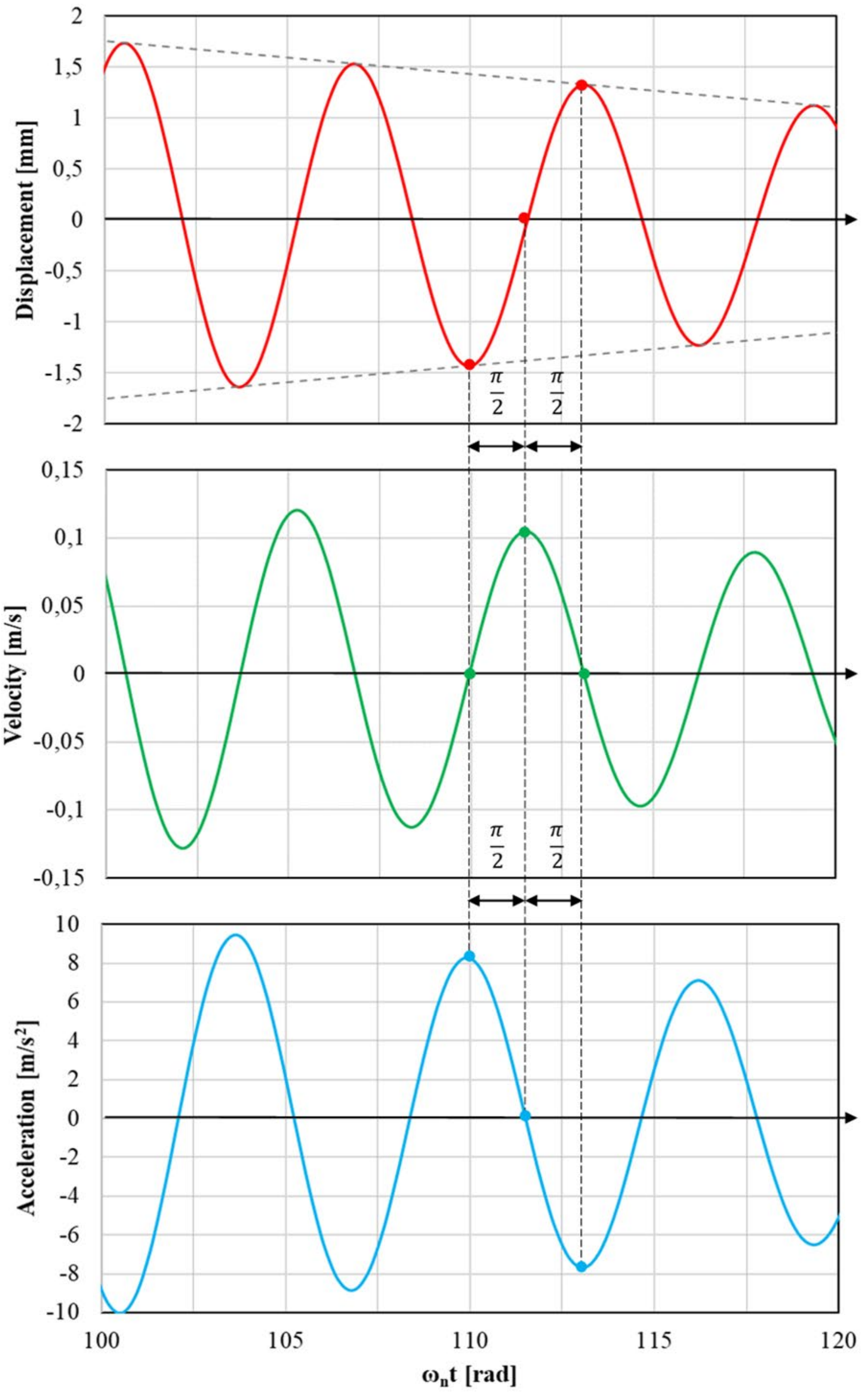

Figure 17: Comparison of transient displacement, velocity, and acceleration responses for the friction damped case. Shows the relationship between the curves.

3.2 Comparisons

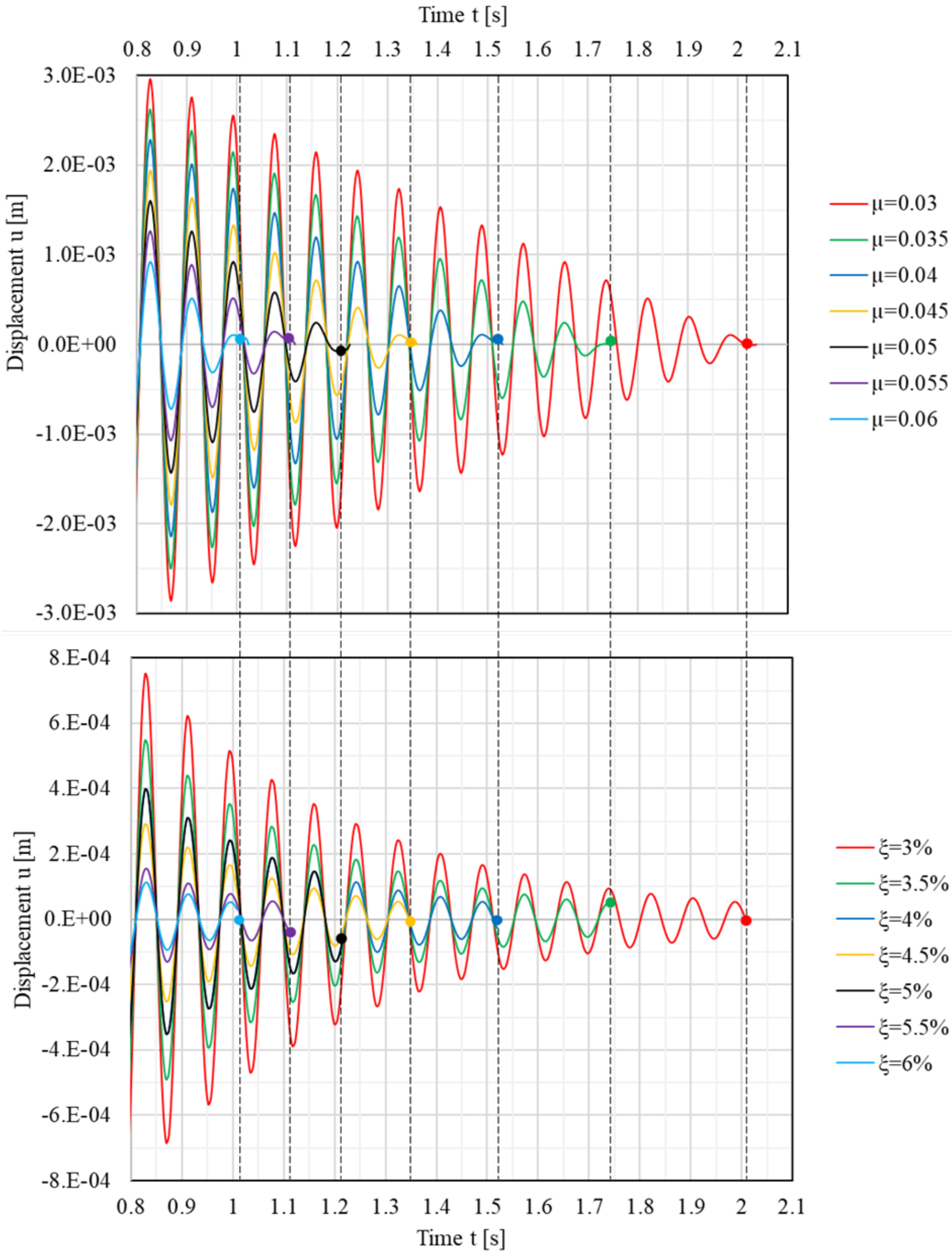

Figure 18: Transient responses of the SDOF system with the different damping values considered for the friction and viscous damped cases. Chosen halting point is indicated and compared for each plot.

Figure 18 illustrates how, during the analysis, it was discovered that for certain values of viscous damping ratios and friction coefficients, the given physical model would effectively return to equilibrium at very similar times in free vibration.

This paper decided that the model would be returned to its equilibrium position at the time interval when its transient displacement response to vibration was less than 0.1mm. This value was selected as displacement values less than this were considered to have negligible effects on the structure. Although for the equivalent friction damped case, the transient response envelope was used to determine when the structure would come to rest in free vibration.

The analysis considered assumed viscous damping ratios between 3-6%, a common assumption range for damping in structures.

It was found that the viscous damping ratio and friction coefficient values that achieved similar displacement responses from the model, the transient responses coming to rest at either the same or very similar times, were essentially equal. The values considered can be seen Table 2 below.

Table 2: Viscous damping ratio and equivalent friction coefficient values that caused the model's transient response to come to rest at similar time intervals.

ξ	0.03	0.035	0.04	0.045	0.05	0.055	0.06
μ	3%	3.5%	4%	4.5%	5%	5.5%	6%

The time and displacement values of the points that were considered as the model's rest position are given in Table 3. The absolute differences between the displacement and time values of the viscous damped (VD) and equivalent friction damped (EFD) cases at the halting points are also shown, calculated as

$$|\boldsymbol{x}_{\boldsymbol{VD}} - \boldsymbol{x}_{\boldsymbol{EFD}}| \tag{26}$$

Note that the transient response halting points have all less than 0.1mm difference between the two damping cases. The largest difference between the transient response values is for $\xi = 5\%$ and $\mu = 0.05$, at 0.084mm. These differences are illustrated by Figure 19.

Table 3: Displacement and time coordinates of the transient (Figure 18), steady-state and total displacement responses at the chosen halting points. The differences between the two damping cases' values are indicated.

Damping Ratio	Friction Coefficient	Transient Response at "end"			Time at "end"		
ξ	μ	Viscous Damping	Equivalent Friction Damping	Difference	Viscous Damping	Equivalent Friction Damping	Difference
		Displacement $u_{tr}(t)$ [mm]			Time t [s]		
3	0.03	-0.011	-0.006	0.005	2.010	2.026	0.016
3.5	0.035	0.048	0.006	0.042	1.741	1.736	0.005
4	0.04	-0.027	0.026	0.053	1.519	1.519	0.000
4.5	0.045	-0.008	0.040	0.048	1.349	1.349	0.000
5	0.05	-0.043	-0.054	0.011	1.209	1.214	0.005
5.5	0.055	-0.024	0.060	0.084	1.106	1.106	0.000
6	0.06	0.014	0.065	0.051	1.013	1.013	0.000
Damping Ratio	**Friction Coefficient**	**Steady State Response at "end"**			**Time at "end"**		
ξ	μ	Viscous Damping	Equivalent Friction Damping	Difference	Viscous Damping	Equivalent Friction Damping	Difference
		Displacement $u_{ss}(t)$ [mm]			Time t [s]		
3	0.03	0.637	0.796	0.159	2.010	2.026	0.016
3.5	0.035	-0.072	0.006	0.078	1.741	1.736	0.005
4	0.04	0.696	0.484	0.212	1.519	1.519	0.000
4.5	0.045	0.629	0.337	0.293	1.349	1.349	0.000
5	0.05	0.714	0.983	0.269	1.209	1.214	0.005
5.5	0.055	-0.739	-0.983	0.244	1.106	1.106	0.000
6	0.06	0.532	0.231	0.301	1.013	1.013	0.000
Damping Ratio	**Friction Coefficient**	**Total Displacement Response at "end"**			**Time at "end"**		
ξ	μ	Viscous Damping	Equivalent Friction Damping	Difference	Viscous Damping	Equivalent Friction Damping	Difference
		Displacement $u(t)$ [mm]			Time t [s]		
3	0.03	0.626	0.790	0.164	2.010	2.026	0.016
3.5	0.035	-0.024	0.012	0.036	1.741	1.736	0.005
4	0.04	0.669	0.510	0.159	1.519	1.519	0.000
4.5	0.045	0.621	0.377	0.245	1.349	1.349	0.000
5	0.05	0.671	0.929	0.258	1.209	1.214	0.005
5.5	0.055	-0.763	-0.924	0.160	1.106	1.106	0.000
6	0.06	0.545	0.296	0.249	1.013	1.013	0.000

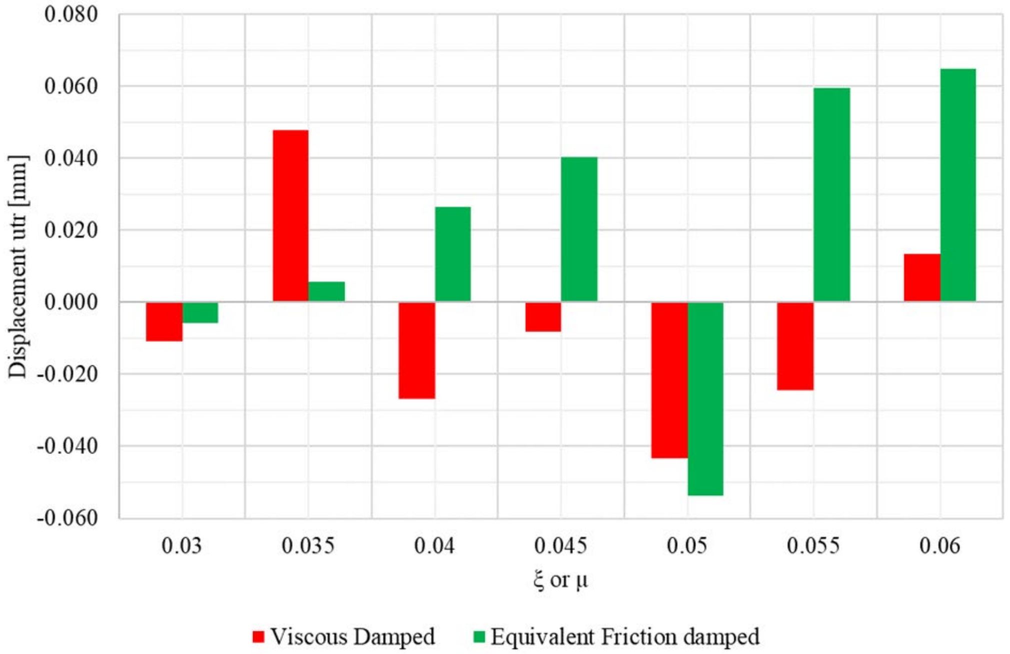

Figure 19: Illustration of the differences between the transient response halting point displacements for the different damping values

Although the differences in displacement values shown in Figure 19 look quite large, they are negligible, none greater than 0.09mm.

3.3 Possible relationship ξ−μ

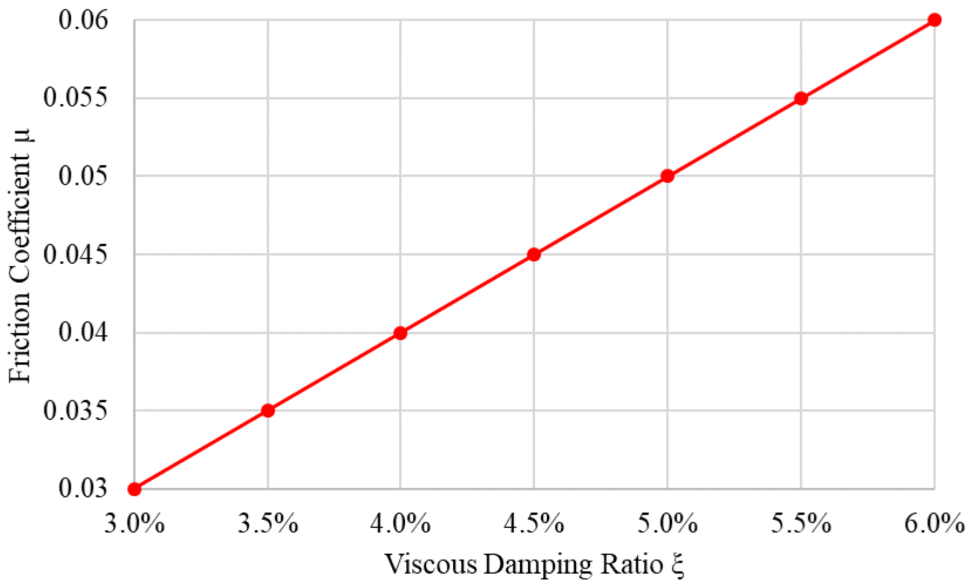

Figure 20: Illustration of a possible viscous damping ratio - friction coefficient relationship

The results of the analysis show that, for this model, there seems to be a linear relationship between the friction coefficient and viscous damping ratio. Figure 20 plots the damping values that yielded similar responses from the model, showing a linear relationship.

4 DISCUSSION

This paper attempted to establish a mathematical relationship between a viscously damped SDOF system, and a friction damped one. The physical model was chosen to represent a typical single-storey structure with realistic parameters.

A theoretical snap-back test was imposed on the model as well as a harmonic excitation force, although the transient vibration response of the model was chiefly considered.

Different values for the friction coefficient and viscous damping ratios were used, keeping those that resulted in similar transient responses from the system. Responses were deemed similar if they reached their equilibrium points at similar time intervals. The equilibrium point was chosen to be when the transient displacement was less than 0.1mm, which the paper considered as a negligible displacement value in the context of structures.

Ultimately this resulted in a linear relationship between the assumed viscous damping ratios and friction coefficients for the selected cases that exhibited similar response.

This paper began with the premise that the common assumption in practice, of a structure having inherent linear viscous damping, was not always correct. This would especially be true in structures with large friction damping forces present, stemming from sources such as seismic friction devices and slip-friction joints in steel members.

This assumption of linear viscous damping is typically made to simplify the calculations instead of using the complicated classical non-linear Coulomb damping. This paper attempted to study the possibility of reducing this complexity by using the alternative method of approximating the friction damping by a harmonic force, proposed by Rizcallah (2019).

The paper expanded the application of this method, deriving displacement, velocity and acceleration response expressions for this alternative approach to friction damping. These expressions were subsequently used in the analysis of the SDOF system when friction damped.

The resulting linear relationship between ξ and μ for the studied SDOF cases implies that the assumption of linear viscous damping in a system may possibly be valid and producing similar results to that of a friction damped system for the studied cases. However, the future analysis should be expanded to consider classical non-linear Coulomb damping and more cases including MDOF systems and different loading conditions. The criteria for which the system's responses in different damping cases are deemed similar should also be re-evaluated with requirements that are more precise in practice.

The purpose of trying to relate the viscous damping ratio and friction coefficient is so that the design and modelling of structures with seismic friction dampers and/or friction forces in structural connections can be done more accurately. Whereas currently the specifics of how accurately seismic design software mathematically models friction damped software is unknown.

5 REFERENCES

Chopra, A. K. (2017). *Dynamics of structures : theory and applications to earthquake engineering* (Fifth edition. ed.). Pearson. https://ezproxy.aut.ac.nz/login?url=https://search.ebscohost.com/login.aspx?direct=true&db=cat05020a&AN=aut.b1971645x&site=eds-live

Ramhormozian, S. (2020, August). Free vibration of damped single degree of freedom systems. ENBU801 Structural Dynamics, Auckland University of Technology.

Rizcallah, J. A. (2019, August 26). Revisiting the coulomb-damped harmonic oscillator. *European Physical Society, 40*(5), Article 055004. https://doi.org/10.1088/1361-6404/ab33d1

Tube, S. (2017). *Design with steel - dimensions and properties handbook* (47, Ed.).